Journal of Biomolecular NMR (2005) 31: 321–330
DOI 10.1007/s10858-005-2039-y

Article

A set of HA-detected experiments for measuring scalar and residual dipolar couplings

Peter Würtz, Kai Fredriksson & Perttu Permi*
NMR Laboratory, Program in Structural Biology and Biophysics, Institute of Biotechnology, University of Helsinki, P.O. Box 65FIN-00014, Helsinki, Finland

Received 2 November 2004; Accepted 2 February 2005

Key words: dipolar couplings, HCACO, NMR, proteins, scalar couplings, spin-state-selection

Abstract

A new set of HCACO based three-dimensional NMR experiments for measuring residual dipolar couplings in proteins is presented. Using spin-state selection and editing in three dimensions, the experiments allow accurate measurement of intraresidual $^1D_{C^\alpha H^\alpha}$, $^1D_{C'C^\alpha}$ and $^2D_{C'H^\alpha}$ scalar and residual dipolar couplings of ^{15}N/^{13}C labeled proteins in D_2O and dilute liquid crystals with minimal spectral crowding. The presented experiments are especially suitable for small or medium sized proline-rich proteins, or proteins that require high pH solvent conditions, making $^1H^N$ detected experiments unattractive. In addition, the tetrahedral coordination of C^α is superior to the planar peptide bond for determination of local alignments in partially structured polypeptides. For the efficient use of spectrometer time and to avoid complications arising from the varying magnitude of the alignment tensor during relatively long experiments, the $^1D_{C^\alpha H^\alpha}$ and $^2D_{C'H^\alpha}$ couplings can also be measured simultaneously in an E.COSY like manner with high accuracy. The pulse sequences are balanced for cross-correlation effects and minimized for relaxation losses. The pulse sequences are tested with a sample of ^{15}N/^{13}C human ubiquitin. We find internuclear vector directions determined from the dipolar couplings to have an excellent correlation with those of ubiquitin's refined solution structure.

Introduction

Residual dipolar couplings (RDCs) induced by a tunable alignment of biological macromolecules in a dilute liquid crystal medium have attracted both structural and dynamical NMR studies of proteins and nucleic acids (Bax and Tjandra, 1997; Tjandra and Bax, 1997; Prestegard et al., 2000; Bax et al., 2001, Annila and Permi, 2004). Not surprisingly, myriad of experiments have been developed for the measurement of dipolar couplings during the past several years (Prestegard et al., 2000; Tjandra and de Alba, 2002; Bax et al., 2001, Prestegard et al. 2004). Our group has earlier developed a suite of NMR experiments for measuring residual dipolar couplings in protein backbone and sidechain (Permi et al., 1999, Permi and Annila, 2000, Permi, 2001, Permi 2003). There are obvious reasons to measure RDCs using the $^1H^N$ detected TROSY based HNCO experiments (Permi et al., 2000a) but in some cases one may encounter a situation where determination of RDCs from $^1H^\alpha$ detected experiments can readily be justified. Firstly, some proteins may require a relatively high pH or temperature, where the amide proton exchange rate with water is too high. These conditions decline the attainable sensitivity on $^1H^N$ detected experiments, especially on studies of flexible systems. In that case, the $^1H^\alpha$ detected *out and back* experiments in D_2O provide a meaningful alternative to accomplish the sequential assignment and to measure residual dipolar couplings. Secondly, lack of RDC information from

*To whom correspondence should be addressed. E-mail: Perttu.Permi@helsinki.fi

non-redundant directions due to the planarity of the peptide bond impairs accurate determination of the alignment tensor for small and α-helical proteins (Clore et al., 1998a, b). It is then advantageous to measure RDCs around the chiral $^{13}C^{\alpha}$ nucleus as its tetrahedral coordination is more favorable than that of the planar peptide bond especially in determination of alignment in a partially structured polypeptide chain. Thirdly, studies of proline-rich polypeptides have provoked the design of novel methodology for the efficient assignment of these proteins (Kanelis et al., 2000). It is obvious that widely used HNCO based experiments are not amenable for residues preceding proline. Although dipolar couplings in these residues can be measured with HNCA based experiment, which provides high sensitivity, the HCACO based pulse schemes are suitable both for prolines and residues preceding prolines. For our recent study on RDCs, applied to probe molecular dynamics of flexible molecules, we used a set of ^{13}C-HSQC based experiments for measuring RDCs in a dilute liquid crystal medium with D_2O as a solvent (Fredriksson et al., 2004). This inspired us to develop suitable NMR methodology for measuring RDCs in protein samples dissolved in 100% D_2O constituting of dilute liquid crystal medium such as bicelles. In this paper, we introduce novel spin-state-selective $^{1}H^{\alpha}$ detected triple-resonance experiments for determination of scalar and residual dipolar couplings in small proteins. The proposed methodology was applied for human ubiquitin, prepared in bicelle medium dissolved in D_2O, and very good correlation with the previously refined NMR structure was obtained (Cornilescu et al., 1998).

Experimental

The novel $^{1}H^{\alpha}$ detected experiments were tested on uniformly $^{15}N/^{13}C$-labeled ubiquitin, constituting of 76 amino acid residues. All scalar couplings were measured on a $\sim$ 1.5 mM sample, dissolved in 99.9% D_2O in a 250 μl Shigemi microcell, pH 6.8, 10 mM potassium phosphate buffer at 30°C (Asla Ltd., Riga, Latvia). For measuring the residual dipolar contribution to the scalar couplings in aligned medium, the protein was prepared into a liquid crystal medium ($\sim$ 3% w/v) constituting of dry 1,2-Di-*O*-dodecyl-*sn*-Glycero-3-Phosphocholine (DMPC) and 1,2-Di-*O*-Hexyl-*sn*-Glycero-3-Phosphocholine (DHPC) phospholipids and cetyltrimethyl ammonium bromide (CTAB) in the ratio 30:10:1 dissolved in 99.9% D_2O. The approximate protein concentration was 1 mM. The corresponding ^{2}H splitting in oriented sample was 11.3 Hz, which was measured using a single pulse ^{2}H experiment in the beginning and after the measurements in order to verify sample stability. All spectra were recorded on a Varian Unity INOVA 600 MHz NMR spectrometer, equipped with a triple-resonance probehead and an actively shielded *Z*-axis gradient system. Spectra were processed and analyzed using the standard VNMR 6.1 revision C software package (Varian associates, 2000).

The HCACO(α/β-*J*-HACA) spectrum in D_2O, recorded with pulse sequence shown in Figure 1a, was collected with 40, 32 and 410 complex points using 4 transients per FID, corresponding to acquisition times of 22.2, 6.4 and 51.1 ms in t_1, t_2, and t_3, respectively. A total experimental time was 10.5 h. Data were zero-filled to $256 \times 256 \times 2048$ points and apodized with shifted squared sine-bell functions in all three dimensions. Experimental parameters for the HCACO(α/β-*J*-HACA) spectrum measured in a dilute liquid crystalline medium were identical to the spectrum measured in D_2O, except for 8 transients used for signal accumulation (experimental time 21 h).

For the HCACO(α/β-*J*-C′CA) spectrum in D_2O (pulse sequence in Figure 1b), 80, 32 and 410 complex points was collected, using 4 transients per FID. The corresponding acquisition times were 44.4, 6.4 and 51.1 ms in t_1, t_2, and t_3, respectively. A total experimental time was 21 h. Data were zero-filled to $512 \times 128 \times 2048$ points and apodized with shifted squared sine-bell functions in all three dimensions. Experimental parameters for the HCACO(α/β-*J*-C′CA) spectrum measured in a dilute liquid crystalline medium were identical to the spectrum measured in D_2O, except for 6 transients used for signal accumulation (experimental time 31.5 h).

The experimental details for the HCACO(α/β-*J*-C′HA) spectrum in D_2O, recorded with the pulse sequence shown in Figure 1c, are as follows: 2 transients were used for collecting 76, 128 and 820 complex points, corresponding to acquisition times of 42, 25.6 and 51.1 ms, in t_1, t_2, and t_3, respectively. A total experimental time was 40 h.

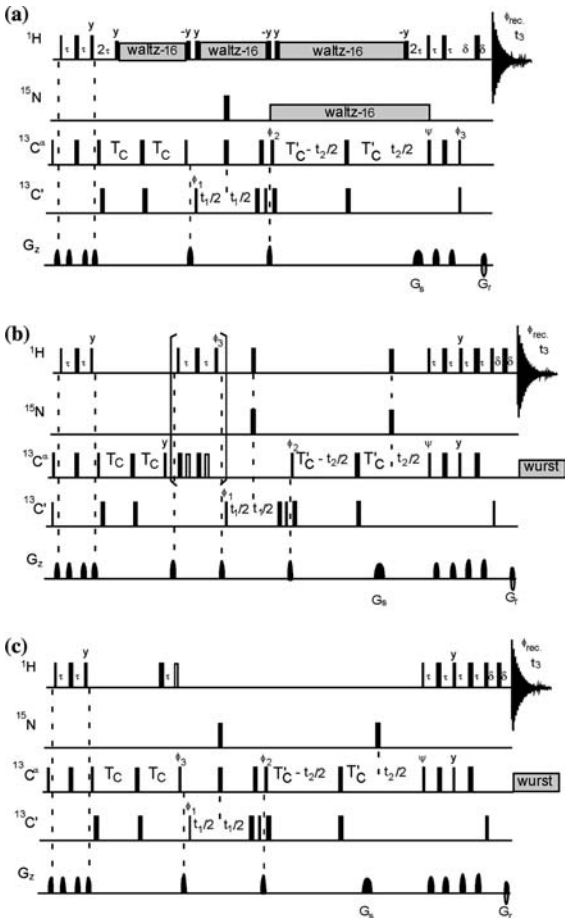

Figure 1. Spin-state-selective HCACO based pulse sequences for the measurement of $^{1}(J+D)_{C^{\alpha}H^{\alpha}}$ (a), $^{1}(J+D)_{C'C^{\alpha}}$ (b), and $^{1}(J+D)_{C^{\alpha}H^{\alpha}}$ and $^{2}(J+D)_{C'H^{\alpha}}$ scalar and residual dipolar couplings in ^{15}N, ^{13}C labeled proteins in D_2O. Narrow (wide) bars correspond to 90° (180°) pulses, with phase x unless otherwise. All 90° (180°) pulses for $^{13}C'$ and $^{13}C^{\alpha}$ are applied with a strength of $\Omega/\sqrt{15}$ ($\Omega/\sqrt{3}$), where Ω is the frequency difference between the centers of the $^{13}C'$ and $^{13}C^{\alpha}$ regions. The ^{1}H, ^{15}N, $^{13}C'$, and $^{13}C^{\alpha}$ carrier positions are 4.7 (HDO), 120 (center of ^{15}N spectral region), 57 ppm (center of $^{13}C^{\alpha}$ spectral region) and 175 ppm (center of $^{13}C'$ spectral region), respectively. All $^{13}C'$ and $^{13}C^{\alpha}$ off-resonance pulses are applied with phase modulation by Ω. The ^{13}C transmitter is initially set to the $^{13}C^{\alpha}$ region, shifted to 175 ppm just before the 90° ϕ_1 pulse, and shifted back to 57 ppm after the 90° ($^{13}C'$)pulse following the t_1 period. Pulsed field gradients are inserted as indicated for coherence transfer pathway selection and residual water suppression. The delays employed are: $\tau = 1/(4J_{CH})$; T_C = ~3.5 ms; T'_C = ~3.5 ms or ~13.5 ms; δ = G_r + field recovery delay. (a) the HCACO(α/β-*J*-HACA) scheme. Phase cycling: $\phi_1 = x, -x$; $\phi_2 = 2(x), 2(-x)$; $\phi_{rec.} = x, 2(-x), x$. The spin-state selection is accomplished by the phase setting of ϕ_3. If ϕ_3 is y or $-y$, either upfield or downfield component of $^{1}J_{C^{\alpha}H^{\alpha}}$ doublet is obtained, respectively. Quadrature detection in the F_1-dimension is obtained by altering the phase of ϕ_1 according to States-TPPI (Marion et al., 1989). For quadrature detection in F_2, two data sets are collected (I): $\psi = x$; (II): $\psi = -x$; with simultaneous change in gradient polarity. The data processing is according to sensitivity enhanced method (Kay et al., 1992). Gradient strengths (durations) are optimized for the highest sensitivity: G_s = 30 G/cm (1 ms), G_r = 29.6 G/cm (0.25 ms). (b) the HCACO(α/β-*J*-C′CA) scheme. All parameters as in (a) except for the phase cycling. For the in-phase spectrum (unfilled 180° pulses on $^{13}C^{\alpha}$ are applied during the filter): $\phi_1 = x, -x$; $\phi_2 = 2(y), 2(-y)$; $\phi_3 = x$; $\phi_{rec.} = x, 2(-x), x$; for the antiphase spectrum (filled 180° pulses on $^{13}C^{\alpha}$ are applied during the filter): $\phi_3 = y$. The in- and antiphase data sets are recorded in an interleaved manner and subsequently added and subtracted to separate the multiplet components into two subspectra. (c) the HCACO(α/β-*J*–C′HA) experiment. All parameters as in (a) except for the phase cycling. For the in-phase spectrum (unfilled 180° pulse on ^{1}H is applied immediately prior to the pulse with phase ϕ_3): $\phi_1 = x, -x$; $\phi_2 = 2(y), 2(-y)$; $\phi_3 = y$; $\phi_{rec.} = x, 2(-x), x$; for the antiphase spectrum (filled 180° pulses on ^{1}H is applied delay τ prior to the pulse with phase ϕ_3): $\phi_3 = x$. The in- and antiphase data sets are recorded in an interleaved manner and subsequently added and subtracted to separate the multiplet components into two subspectra.

Data were zero-filled to $512 \times 512 \times 1024$ points and apodized with shifted squared sine-bell functions in all three dimensions. Experimental parameters for the HCACO(α/β-*J*-C′HA) spectrum measured in a dilute liquid crystalline medium were identical to the spectrum measured in D_2O, except for 4 transients used for signal accumulation (experimental time 80 h).

Results and discussion

Method for measuring $^{1}J_{H^{\alpha}C^{\alpha}}$

The HCACO(α/β-*J*-HACA) pulse scheme proposed for measuring $^{1}(J+D)_{H^{\alpha}C^{\alpha}}$ is depicted in Figure 1a. It is essentially similar to the familiar HCACO experiment (Kay et al., 1990) and to the spin-state-selective HCACO-α/β experiment (Andersson et al., 1998). The coherence transfer can be described as follows

$$^{1}H^{\alpha}(i) \xrightarrow{^{1}J_{CH}} {}^{13}C^{\alpha}(i) \xrightarrow{^{1}J_{C'C^{\alpha}}} {}^{13}C'(i)(t_1)$$
$$\xrightarrow{^{1}J_{C'C^{\alpha}}} {}^{13}C^{\alpha}(i)(CT - t_2) \xrightarrow{^{1}J_{CH}} {}^{1}H^{\alpha}(i)(t_3)$$

where the active couplings are indicated above the arrows, and $t_{1\text{-}3}$ are acquisition times. Initially, the magnetization is transferred from the $^{1}H^{\alpha}(i)$ spin to the directly bound $^{13}C^{\alpha}(i)$ spin. This step is followed by the $^{13}C^{\alpha}(i)$–$^{13}C'(i)$ transfer utilizing the relatively large $^{1}J_{C^{\alpha}C'}$ coupling. During this period,

the desired coherence is also modulated by $^1J_{C^\alpha C^\beta}$ coupling and diminished by the transverse relaxation. There are different options to transfer magnetization from $^{13}C^\alpha(i)$ to$^{13}C'(i)$ (Permi and Annila, 2004) but we chose the conventional INEPT transfer. Subsequently, the chemical shift of $^{13}C'(i)$ spin is recorded during the t_1 period. Identical but reverse transfer step is used for refocusing the $^{13}C^\alpha$ antiphase coherence while the labeling of the $^{13}C^\alpha(i)$ chemical shift takes place during the t_2 period. Ultimately, the magnetization is converted back to $^1H^\alpha(i)$ single quantum coherence by the coherence order selective spin-state-selective filter (Parella and Belloc, 2001, Permi, 2002). In short, depending on the phase of the final 90° (^{13}C) pulse, either the upfield or downfield component of the $^1H^\alpha$–$^{13}C^\alpha$ doublet is selected (Permi, 2002). Thus, for measuring $^1(J+D)_{H^\alpha C^\alpha}$ couplings, two data sets are recorded with $\phi_3 = y$, $-y$, This results in two spin-state edited spectra, exhibiting correlations at $\omega_{C'}(i)$, $\omega_{C^\alpha}(i)$, $\omega_{H^\alpha}(i)$ $+\pi^1(J+D)_{H^\alpha C^\alpha}$ and $\omega_{C'}(i)$, $\omega_{C^\alpha}(i)$, $\omega_{H^\alpha}(i) - \pi^1(J$ $+D)_{H^\alpha C^\alpha}$, enabling measurement of $^1(J+D)_{H^\alpha C^\alpha}$ from the cross peak displacement in F_3 dimension between two spin-state edited spectra. It is worth pointing out that the proposed experiment is a gradient selected and sensitivity enhanced spin-state-selective HCACO experiment. It thus provides an inherent sensitivity improvement by a factor of $\sqrt{2}$ with respect to the HCACO-α/β scheme (Andersson et al., 1998) as both orthogonal magnetization components are transferred from $^{13}C^\alpha$ back to $^1H^\alpha$ (Permi, 2002). Remarkably, the proposed sequence is also shorter by 4Δ–2δ than the scheme introduced by Andersson and co-workers. However, spin-state selection is not obtained for glycine residues. For optimal detection of glycines, the ^1H composite pulse decoupling should be omitted, whereas phase of the $90_{\phi 3}(^{13}C^\alpha)$ should be set to x or $-x$. This phase setting removes the dipole–dipole cross-correlation between the geminal proton pair, enabling accurate determination of $^1(J+D)_{H^\alpha C^\alpha}$ couplings in I_2S moieties (Permi, 2002).

Method for measuring $^1J_{C'C^\alpha}$

Dipolar coupling between the $^{13}C^\alpha$ and $^{13}C'$ spins is one order of magnitude smaller than the dipolar contribution between the $^{13}C^\alpha$ and $^1H^\alpha$ spins. Several experimental schemes can be employed for probing the orientation of $^{13}C^\alpha$–$^{13}C'$ bond vector (Permi et al. 1999; Yang et al., 1999; Permi et al. 2000a; Giesen et al., 2002). In $^1H^\alpha$-detected methodology, constant-time ^{13}C-HSQC experiment has been applied for measuring $^1J_{C'C^\alpha}$ from the $^{13}C^\alpha$ -dimension (Vuister and Bax, 1992). We propose measurement of this coupling from the $^{13}C'$-dimension by utilizing spin-state-selective filtering. The proposed HCACO(α/β- J-C′CA) scheme is shown in Figure 1b. The flow of coherence follows mainly the HCACO pathway

$$^1H^\alpha(i) \xrightarrow{^1J_{CH}} {}^{13}C^\alpha(i) \xrightarrow{^1J_{C'C^\alpha}} {}^{13}C'(i)(t_1) \xrightarrow{^1J_{C'C^\alpha}} {}^{13}C^\alpha(i)(CT - t_2) \xrightarrow{^1J_{CH}} {}^1H^\alpha(i)(t_3)$$

The couplings used for transfer are shown above the arrows, and $t_{1\text{-}3}$ corresponds to acquisition times. The experiment is conceptually similar to our previously described HNCO(α/β- J-NC′) schemes (Permi et al., 1999; Permi et al., 2000a). In this case, the magnetization is first transferred from $^1H^\alpha(i)$ to $^{13}C^\alpha(i)$ utilizing the INEPT transfer. Transfer step from $^{13}C^\alpha(i)$ to $^{13}C'(i)$ follows except that composite pulse proton decoupling is not applied during the $^{13}C^\alpha$–$^{13}C'$ INEPT as in the HCACO(α/β-J-HACA) scheme. The spin-state-selective filter is incorporated into the pulse sequence prior to the t_1 evolution period (indicated with brackets in Figure 1b). Hence, two different data sets per t_1 value are recorded. The first data set, corresponding to the in-phase spectrum, is recorded with two 180° ($^{13}C^\alpha$) pulses (marked with unfilled bars) applied at the midpoints of delays τ in order to retain the desired coherence in-phase with respect to the $^{13}C^\alpha(i)$ spin prior the t_1 period. The second data set, corresponding to the antiphase spectrum, is recorded with two 180° ($^{13}C^\alpha$) pulses (marked with filled bars) applied immediately after 90° (^1H) and 180° (^1H) pulses, respectively. In addition, the phase of the $90_{\phi 3}(^1H)$ pulse is shifted by 90° with respect to the preceding 90° (^1H) pulse. The following gradient pulse dephases any undesired dispersive magnetization originating from J-mismatch (Permi et al., 2000b). The cross-correlation between chemical shielding anisotropy (CSA) of $^1H^\alpha$ and dipole–dipole relaxation (DD) of $^{13}C^\alpha$–$^1H^\alpha$ is averaged by equalizing the relaxation rates of doublet components by the inversion of $^{13}C^\alpha$s spin-state during the filter elements.

The $^{1}(J+D)_{C'C^{\alpha}}$ coupling evolves during t_1 simultaneously with the $^{13}C'(i)$ chemical shift. Subsequently, the preferred coherence is transferred back to the $^{13}C^{\alpha}(i)$ spin and its chemical shift is labeled during the t_2 evolution period implemented into the $2T'_C$ back-transfer step. Ultimately, the gradient selected, sensitivity enhanced INEPT transfer (Kay et al., 1992) is utilized for converting magnetization back to $^{1}H^{\alpha}$ coherence.

Two subspectra displaying cross peaks at $\omega_{C'}(i)+\pi^{1}(J+D)_{C'C^{\alpha}}, \omega_{C^{\alpha}(i)}, \omega_{H^{\alpha}}(i)$ and $\omega_{C'}(i)-\pi^{1}(J+D)_{C'C^{\alpha}}, \omega_{C^{\alpha}}(i), \omega_{H^{\alpha}}(i)$ will be obtained after appropriate addition and subtraction of in- and antiphase data sets. The $^{1}(J+D)_{C'C^{\alpha}}$ couplings can be readily measured from the cross peak displacement in $^{13}C'$ dimension between two subspectra exhibiting minimal resonance overlap.

Method for simultaneous measurement of $^{2}J_{C'H^{\alpha}}$ and $^{1}J_{C^{\alpha}H^{\alpha}}$,

The inherently smaller two-bond scalar coupling between $^{1}H^{\alpha}(i)$ and $^{13}C'(i)$ spins has been shown to correlate moderately with the Ramachandran angle ψ, although other factors have a significant influence on $^{2}J_{C'H^{\alpha}}$ (Vuister and Bax, 1992). The sign of scalar $^{2}J_{C'H^{\alpha}}$ is negative (Vuister and Bax, 1992). Residual dipolar contribution to the measured splitting between the $^{1}H^{\alpha}(i)$ and $^{13}C^{\alpha}(i)$ spins is on the order of 7 Hz (assuming $D_a^{CH}=40$ Hz) making this coupling very useful for protein structure determination providing that RDCs between the $^{1}H^{\alpha}(i)$ and $^{13}C^{\alpha}(i)$ spins can be measured with a sufficient accuracy. This coupling has earlier been measured from a two-dimensional constant-time ^{13}C-HSQC spectrum by omitting $^{13}C'$ decoupling during t_1 and acquisition (Vuister and Bax, 1992). If the $^{13}C'$ spin-state is not perturbed between the acquisition periods, a familiar E.COSY pattern emerges, facilitating the measurement of $^{2}(J+D)_{C'H^{\alpha}}$ coupling from the ^{1}H dimension. However, signal dispersion in the resulting two-dimensional $^{1}H^{\alpha}$–$^{13}C^{\alpha}$ correlation map is rather modest, especially if the spin-state-selective filtering is not utilized for removing unnecessary spectral crowding. In addition, as $^{2}D_{C'H^{\alpha}}$ is small in comparison to $D_{H^{\alpha}H^{i}}$ (where i corresponds to adjacent aliphatic protons) and to the $^{1}H^{\alpha}$ linewidth, the experimental error can be significant. For these reasons, we have chosen to determine $^{2}(J+D)_{C'H^{\alpha}}$ from the $^{13}C'$ dimension, where linewidth is much smaller and unresolved residual homonuclear dipolar couplings contribute lineshape to a lesser extend.

The HCACO(α/β-*J*-C′HA) experiment is presented in Figure 1c. The magnetization is transferred through the experiment in the following way

$$^{1}H^{\alpha}(i) \xrightarrow{^{1}J_{CH}} {}^{13}C^{\alpha}(i) \xrightarrow{^{1}J_{C'C^{\alpha}}} {}^{13}C'(i)(t_1) \xrightarrow{^{1}J_{C'C^{\alpha}}} {}^{13}C^{\alpha}(i)(CT-t_2) \xrightarrow{^{1}J_{CH}} {}^{1}H^{\alpha}(i)(t_3)$$

Active couplings used for transferring the coherence are shown above the arrows, and t_{1-3} corresponds to acquisition times. After the initial INEPT transfer, the magnetization is relayed from $^{13}C^{\alpha}(i)$ to $^{13}C'$ (i) during $2T_C$. The spin-state selection is obtained in a manner that is similar to the recipe introduced by Bax and co-workers (Ottiger et al., 1998). To this end, two data sets are recorded per t_1 increment. For the in-phase data set, a 180° (^{1}H) pulse (marked with an unfilled bar) is applied immediately before the $90°_{\phi 3}(^{13}C^{\alpha})$ pulse. The corresponding antiphase data set is recorded with a 180° (^{1}H) pulse (marked with a solid bar) applied the delay τ earlier than in the in-phase data set. In addition, the phase of the $90°_{\phi 3}$ ($^{13}C^{\alpha}$) pulse is shifted by 90° with respect to the preceding 90° ($^{13}C^{\alpha}$) pulse. The ensuing gradient pulse removes any undesired dispersive component of magnetization prior to the t_1 evolution period. The $^{13}C'$ chemical shift is recorded during t_1. The small $^{2}(J+D)_{C'H^{\alpha}}$ coupling evolves concomitantly during t_1 as no ^{1}H decoupling is applied. Although the coupling is smaller than the linewidth, the spin-state selection enables an accurate determination of $^{2}(J+D)_{C'H^{\alpha}}$. Subsequently, the coherence is converted back to $^{13}C^{\alpha}(i)$ antiphase magnetization and transferred back to the $^{1}H^{\alpha}(i)$ spin. The chemical shift of the $^{13}C^{\alpha}(i)$ spin is labelled during the t_2 evolution delay. As the magnitude of $^{2}D_{H^{\alpha}C'}$ coupling is often larger than $^{2}J_{C'H^{\alpha}}$, we deliberately allow the $^{1}(J+D)_{C^{\alpha}H^{\alpha}}$ coupling to evolve during t_2. In this way, the sign of $^{2}D_{C'H^{\alpha}}$ can readily be resolved by simply inspecting the slope of the line connecting the emerging E.COSY pattern.

After appropriate addition and subtraction of in-phase and antiphase data sets, followed by Fourier transform, the HCACO(α/β-*J*-C′HA) pulse scheme produces two three-dimensional subspectra, exhibiting cross peaks at

$\omega_{C'}(i)+\pi^2(J+D)_{C'H^\alpha}, \omega_{C^\alpha}(i)+\pi^1(J+D)_{C^\alpha H^\alpha}, \omega_{H^\alpha}(i)$ and $\omega_{C'}(i)+\pi^2(J+D)_{C'H^\alpha}, \omega_{C^\alpha}(i)-\pi^1(J+D)_{C^\alpha H^\alpha}, \omega_{H^\alpha(i)}$ where the $^2(J+D)_{C'H^\alpha}$ couplings can readily be measured from the cross peak displacement along the ^{13}C' dimension between two subspectra. The $^1(J+D)_{C^\alpha H^\alpha}$ couplings can be measured in an analogous manner along the $^{13}C^\alpha$ dimension, if the acquisition time in t_2 is sufficiently long (> 10 ms). In that case, the delay $2T'_C$ should be set to 27 ms, or alternatively a semi-constant time evolution could be utilized (Logan et al., 1993). We noticed, not surprisingly, that the measurement of $^1(J+D)_{H^\alpha C^\alpha}$ from the directly detected proton dimension using the HCACO(α/β-*J*-HACA) experiment (Figure 1a) gave somewhat higher *Q* values than the measurement from the $^{13}C^\alpha$ dimension using the HCACO(α/β-*J*-C′HA) pulse scheme (*vide infra*). In this respect, it is advantageous to measure $^1(J+D)_{C^\alpha H^\alpha}$ and $^2(J+D)_{C'H^\alpha}$ couplings from the spin-state selective HCACO(α/β-*J*-C′HA) experiment simultaneously, providing that the transverse relaxation time of the $^{13}C^\alpha$ spin enables use of longer constant-time period for the $^{13}C'$–$^{13}C^\alpha$ back transfer step. This also ensures internal consistency between different residual dipolar couplings even if the sample orientation fluctuates over time (de Alba and Tjandra, 2002). Quite large number of time points has to be acquired for both indirect dimensions (See *experimental*). Especially if long acquisition time is used to measure $^1(J+D)_{C^\alpha H^\alpha}$, the total experimental time can be rather long. This can be circumvented by downscaling the chemical shift of $^{13}C'$ with respect to the $^2(J+D)_{C'H^\alpha}$ coupling (Permi et al., 2000) or by shortening the acquisition time for $^1(J+D)_{C^\alpha H^\alpha}$ coupling evolution. Owing to the large dynamic range of $^1D_{C^\alpha H^\alpha}$ dipolar contribution, an acquisition time of 10–15 ms is sufficient for the accurate measurement of $^1D_{C^\alpha H^\alpha}$ (Yang et al., 1998; Permi, 2003).

Although not tested in our case, it has been shown that the multiple-quantum coherence between $^{13}C^\alpha$ and $^1H^\alpha$ spins may have more favorable relaxation properties in comparison to $^{13}C^\alpha$ single-quantum coherence (Griffey and Redfield, 1987; Grzesiek and Bax, 1995). To this end, the proposed experiments can be devised in such a way that relatively weak rf field strength is used for spinlocking of $^1H^\alpha$ spins during the heteronuclear transfer steps while heteronuclear multiple-quantum coherence is maintained throughout the most of the $^{13}C^\alpha$–$^{13}C'$ transfer steps (See supplementary material for details).

Application to human ubiquitin

The proposed methodology was exposed to experimental verification on human ubiquitin, a small 8.6 kDa protein that has been extensively studied by NMR spectroscopy. Figure 2 shows an expansion of residue lys27 in HCACO(α/β-*J*-HACA) (a, a′), HCACO(α/β-*J*-C′CA) (b, b′) and HCACO(α/β-*J*-C′HA) (c, c′) spectra, recorded in D_2O (left panels) and in aligned medium constituting of phospholipid bilayers aka bicelles in D_2O (right panels). In each case, the spin-state edited subspectra are overlaid for the sake of clarity. The doublet components corresponding to either upfield or downfield spin-state are shown with thin or thick contours, respectively. The measured scalar couplings in D_2O and the corresponding $(J+D)$ values in the oriented sample are indicated by arrows. As can be seen from Figure 2c, c′, the slope of the line between the E.COSY multiplet components changes its sign due to the rather large residual dipolar contribution into the measured $^2J_{C'H^\alpha}$ value. This can easily be recognized as we permit the $^1H^\alpha$ (*i*) spin to interact with both the $^{13}C'(i)$ and $^{13}C^\alpha(i)$ spins during t_1 and t_2, respectively.

The measured dipolar couplings were fitted to ubiquitin's refined NMR structure (PDB code: 1D3Z) using the singular value decomposition method (Losonzci et al., 1999) implemented in the software package PALES (Zweckstetter and Bax, 2000). Best fits between the measured $^1D_{H^\alpha C^\alpha}$, $^1D_{C'C^\alpha}$, and $^2D_{C'H^\alpha}$ residual dipolar couplings and the ubiquitin refined NMR structure

Figure 2. Expansions of HCACO(α/β-*J*-HACA) (a–a′) HCACO(α/β-*J*-C′CA) (b–b′) and HCACO(α/β-*J*-C′HA) (c-c′) spectra of lys27 residue in ubiquitin. The up- and downfield doublet components, separated into subspectra, are shown overlaid with thick and thin contours. The spectra shown in left panels were recorded from 1 mM uniformly ^{15}N, ^{13}C-labeled ubiquitin in D_2O, whereas the panels in right correspond to spectra recorded from 0.6 mM ubiquitin, dissolved in liquid crystal medium. The spectra a and a' show an $^1J_{C^\alpha H^\alpha}$ and $^1(J+D)_{C^\alpha H^\alpha}$ splitting for lys27, whereas spectra b and b′ show the $^1J_{C'C^\alpha}$ and $^1(J+D)_{C'C^\alpha}$ splitting along the $^{13}C'$ dimension for the corresponding residue. The $^1J_{C^\alpha H^\alpha}$ and $^1(J+D)_{C^\alpha H^\alpha}$, and $^2J_{C'H^\alpha}$ and $^2(J+D)_{C'H^\alpha}$ splittings can be measured readily along the $^{13}C^\alpha$, and $^{13}C'$ dimensions in a HCACO(α/β-*J*-C′HA) spectrum shown in c and c′.

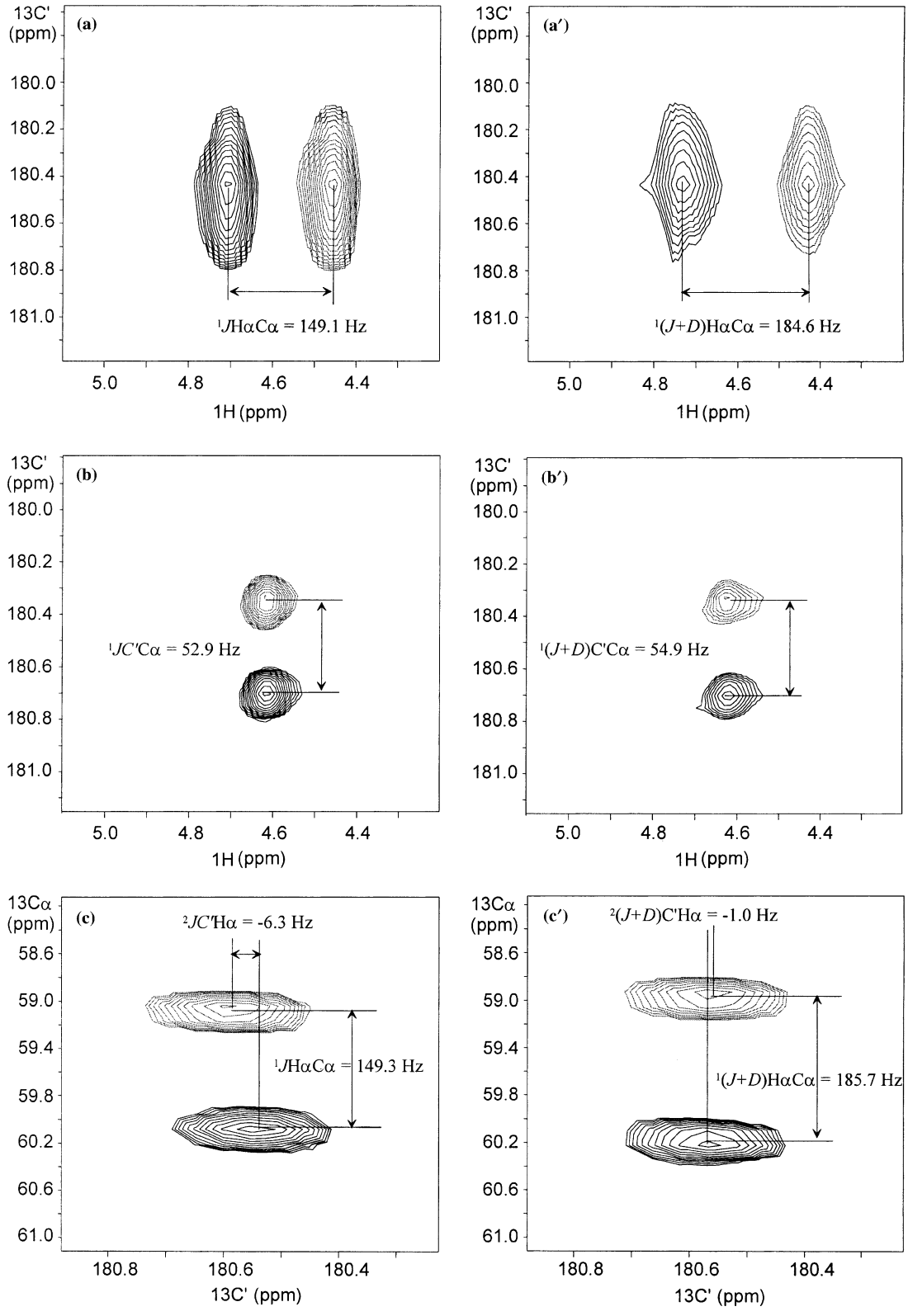
13C' (ppm)
(a)
180.0
180.2
180.4
180.6
180.8
181.0
^1JHαCα = 149.1 Hz
5.0
4.8
4.6
4.4
1H (ppm)
(a′)
$^1(J+D)$HαCα = 184.6 Hz
(b)
^1JC'Cα = 52.9 Hz
(b′)
$^1(J+D)$C'Cα = 54.9 Hz
13Cα (ppm)
(c)
^2JC'Hα = -6.3 Hz
^1JHαCα = 149.3 Hz
58.6
59.0
59.4
59.8
60.2
60.6
61.0
180.8
180.6
180.4
13C' (ppm)
(c′)
$^2(J+D)$C'Hα = -1.0 Hz
$^1(J+D)$HαCα = 185.7 Hz

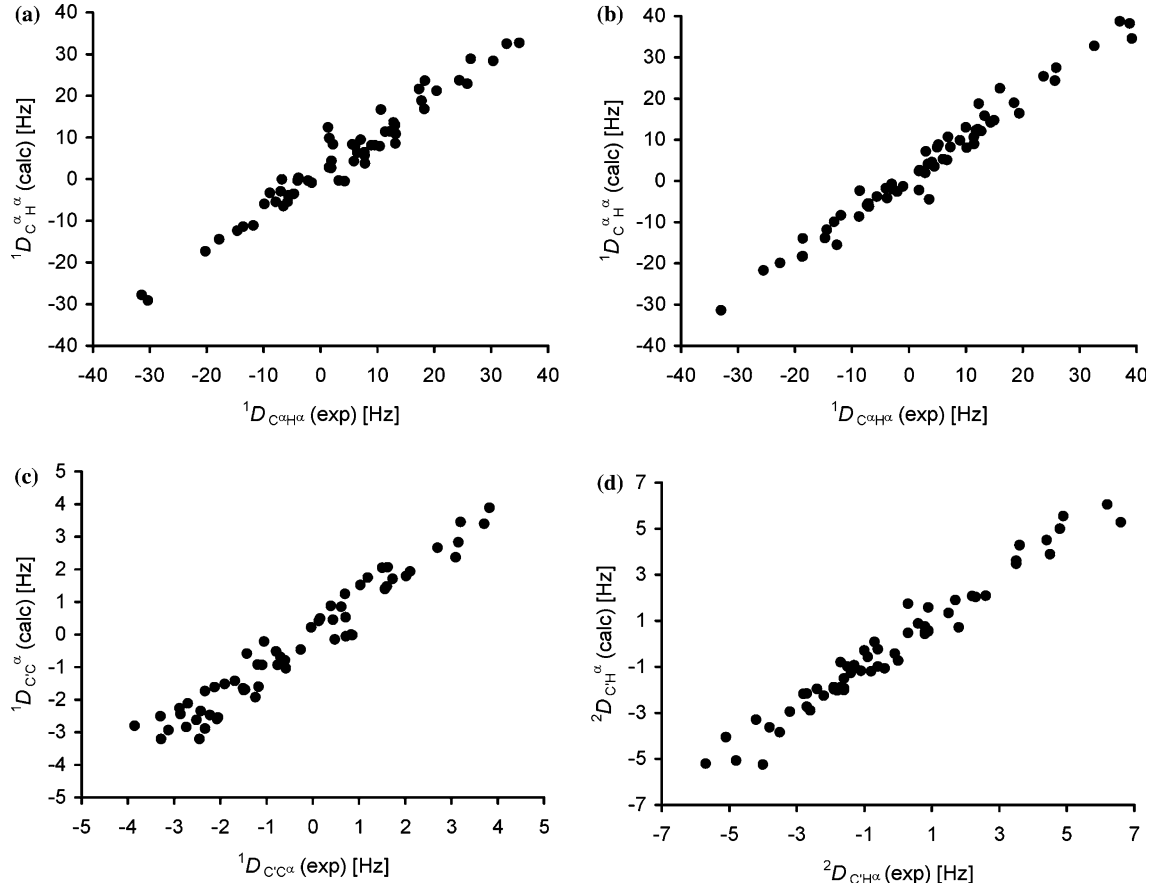

Figure 3. Correlation between the measured $^1D_{C^\alpha H^\alpha}$ (method 1) (a) $^1D_{C^\alpha H^\alpha}$ (method 2) (b) $^1D_{C'C^\alpha}$ (c) and $^2D_{C'H^\alpha}$ (d) residual dipolar couplings with the theoretical couplings values calculated based on ubiquitin lowest energy NMR structure 1D3Z (Cornilescu et al., 1998) using program PALES (Zweckstetter and Bax, 2000). The corresponding Q values are 0.23, 0.17, 0.23 and 0.19, respectively.

are shown in Figure 3a-d, respectively. The corresponding linear correlation coefficients between the measured and predicted RDCs are 0.98 (Q = 0.23), 0.99 (Q = 0.17), 0.97 (Q = 0.23) and 0.98 (0.19) for $^1D_{H^\alpha C^\alpha}$ (method 1, HCACO(α/*β*-*J*-HACA)), $^1D_{H^\alpha C^\alpha}$ (method 2, HCACO(α/*β*-*J*-C′HA)), $^1D_{C'C^\alpha}$, and $^2D_{C'H^\alpha}$, respectively. Glycines as well as the residues in the ubiquitin's flexible tail were not included to the fit. In addition, lys11, leu15, ala28 and asp39 residues were missing in some spectra in liquid crystal medium.

The cross-correlation between $^{13}C^\alpha$–$^1H^\alpha$ and $^1H^\alpha$–$^1H^i$ dipole–dipole interactions can cumulate in the aligned phase, leading to a poorer accuracy if $^1D_{H^\alpha C^\alpha}$ couplings are measured from the $^{13}C^\alpha$ dimension utilizing constant time evolution period with respect to the real time evolution period (Yang et al., 1998). Interestingly, Andersson and co-workers found that the $^1J_{H^\alpha C^\alpha}$ couplings could be measured with higher accuracy along the $^1H^\alpha$ dimension than along the (real time) $^{13}C^\alpha$ dimension (Andersson et al., 1998). Our data suggest that $^1D_{H^\alpha C^\alpha}$ couplings can be measured more accurately from the constant-time ^{13}C dimension than from the $^1H^\alpha$ dimension. This is governed mainly by the unresolved homonuclear ^1H–^1H dipolar couplings hampering the lineshape in the $^1H^\alpha$ dimension.

The spin-state-selective HCACO experiments are prone to the same experimental errors as their HNCO detected counterparts (Permi et al., 2000a). Incomplete suppression of the undesired spin-state may occur if the true coupling value does not exactly match the value used for tuning the spin-state-selective filter (Meissner et al., 1997;

Andersson et al. 1998; Permi et al., 1999). The $^{1}J_{C^{\alpha}H^{\alpha}}$ filter used in the HCACO experiments is tolerant of J leakage (3% threshold) within the mismatch of ± 30 Hz from the tuned value (Yang et al., 1998; Permi et al., 2000b). In the proposed experiments, utilizing the filtering with respect to $^{1}J_{C^{\alpha}H^{\alpha}}$, the J cross talk may occur as the measured $^{1}(J+D)_{C^{\alpha}H^{\alpha}}$ splittings varied between 105–186 Hz. In our case, the potential J mismatch would have had an effect only on the determination of $^{2}D_{C'H^{\alpha}}$ if HCACO(α/β-J-C′HA) had been recorded as a two-dimensional $^{13}C'$, $^{1}H^{\alpha}$ correlation experiment. As the $^{1}(J+D)_{C^{\alpha}H^{\alpha}}$ and $^{1}(J+D)_{C'C^{\alpha}}$ couplings are significantly larger than linewidth, J crosstalk will only be harmful in the case of overlapping α and β states between two different residues.

The signal to noise ratio for ubiquitin was very good. On average, the S/N ratios of 110, 120, and 80 for the HCACO(α/β-J-HACA), HCACO(α/β-J-C′CA), and HCACO(α/β-J-C′HA) experiments was retrieved, respectively. According to Bax and co-workers, an estimate of the attainable lower limit of precision of the measurement can be calculated $\Delta J = \mathrm{LW/SN}$, where ΔJ is the root-mean-square uncertainty, LW is the linewidth at half height and SN stands for the signal to noise ratio (Bax et al., 2001). In the case of small protein like ubiquitin, the linewidths in the $^{13}C'$, $^{13}C^{\alpha}$ and $^{1}H^{\alpha}$ dimensions are small. This yields the accuracy of a fraction of hertz for the measured couplings. In the case of $^{1}(J+D)_{C^{\alpha}H^{\alpha}}$, measured in the $^{13}C^{\alpha}$ dimension, the precision is mainly governed by the constant acquisition time, typically limited to 27 ms in F_2.

Conclusions

We have introduced a new set of spin-state-selective HCACO correlation experiments for measuring scalar and residual dipolar couplings in protein main-chain. The proposed experiments are especially suitable for small or medium sized proline-rich proteins, or proteins that require high pH solvent conditions, making $^{1}H^{N}$ detected experiments unattractive. We have shown that the proposed methodology for measuring residual dipolar couplings in a dilute liquid crystal medium prepared in D_2O solution provides high quality data and the measured RDCs show an excellent correlation to the ubiquitin's refined NMR structure. Measurements of several residual dipolar couplings using the spin-state selective 3D HCACO spectra provide a wealth of structural data information that is highly complementary to the more conventional set of couplings available at the peptide bond e.g. 3D HNCO measurements (Yang et al., 1999; Permi et al., 2000a). The tetrahedral coordination of C^{α} is better than the planar peptide bond, in particular in determination of local alignments in weakly or partially structured polypeptides. We thus believe that the presented experiments can be very useful for protein structure determination as well as for studying structure and dynamics of flexible systems (Louhivuori et al., 2004; Fredriksson et al., 2004).

Supplementary material

One figure describing HCACO based experiments that utilize multiple-quantum coherence during ^{13}C–^{13}C transfer steps Figure 4, available in electronic format at http://dx.doi.org/10.1007/s10858-005-2039-y.

Acknowledgements

We thank the Academy of Finland for financial support.

References

Annila, A., and Permi, P. (2004) *Concepts Magn. Reson.*, **23**, 22–37.

Andersson, P., Weigelt, J., and Otting, G. (1998) *J. Biomol. NMR*, **12**, 435–441.

Bax, A., and Tjandra, N. (1997) *J. Biomol. NMR*, **10**, 289–292.

Bax, A., Kontaxis, G., and Tjandra, N. (2001) *Methods Enzymol.*, **339**, 127–174.

Clore, G.M., Gronenborn, A.M., and Tjandra, N. (1998a) *J. Magn. Reson.*, **131**, 159–162.

Clore, G.M., Gronenborn, A.M., and Bax, A. (1998b) *J. Magn. Reson.*, **133**, 216–221.

Cornilescu, G., Marquardt, J.L., Ottiger, M., and Bax, A. (1998) *J. Am. Chem. Soc.*, **120**, 6836–6837.

Alba, E.de, and Tjandra, N. (2002) *Prog. Nuc. Magn. Reson. Spectrosc.*, **40**, 175–197.

Fredriksson, K., Louhivuori, M., Permi, P., and Annila, A. (2004) *J. Am. Chem. Soc.*, **126**, 12646–12650.

Giesen, A.W., Bae, L.C., Barrett, C.L., Chyba, J.A., Chaykovsky, M.M., Cheng, M.C., Murray, J.H., Oliver, E.J.,

Sullivan, S.M., Brown, J.M., and Homans, S.W. (2002) *J. Biomol. NMR*, **22**, 21–26.
Griffey, R.H., and Redfield, A.G. (1987) *Q. Rev. Biophys.*, **19**, 51–57.
Grzesiek, S., and Bax, A. (1995) *J. Biomol. NMR*, **6**, 335–340.
Kanelis, V., Donaldson, L., Muhandiram, D.R., Rotin, D., Forman-Kay, J.D., and Kay, L.E. (2000) *J. Biomol. NMR*, **16**, 253–259.
Kay, L.E., Ikura, M., Tschudin, R., and Bax, A. (1990) *J. Magn. Reson.*, **89**, 496–501.
Kay, L.E., Keifer, P., and Saarinen, T. (1992) *J. Am. Chem. Soc.*, **114**, 10663–10665.
Logan, T.M., Olejniczak, E.T., Xu, X.R., and Fesik, S.W. (1993) *J. Biomol. NMR*, **3**, 225–231.
Losonczi, J.A., Andrec, M., Fischer, M.W.F., and Prestegard, J.H. (1999) *J. Magn. Reson.*, **138**, 334–342.
Louhivuori, M., Fredriksson, K., Pääkkönen, K., Permi, P., and Annila, A. (2004) *J. Biomol. NMR*, **29**, 517–524.
Marion, D., Ikura, M., Tschudin, R., and Bax, A. (1989) *J. Magn. Reson.*, **85**, 393–399.
Meissner, A., Duus, J.Ø., and Sørensen, O.W. (1997) *J. Biomol. NMR*, **10**, 89–94.
Ottiger, M., Delaglio, F., and Bax, A. (1998) *J. Magn. Reson.*, **131**, 373–378.
Parella, T., and Belloc, J. (2001) *J. Magn. Reson.*, **148**, 78–87.
Permi, P., Sorsa, T., Kilpeläinen, I., and Annila, A. (1999) *J. Magn. Reson.*, **141**, 44–51.
Permi, P., and Annila, A. (2000) *J. Biomol. NMR*, **16**, 221–227.
Permi, P., Rosevear, P.R., and Annila, A. (2000a) *J. Biomol. NMR,*, **17**, 43–54.
Permi, P., Kilpeläinen, I., and Annila, A. (2000b) *J. Magn. Reson.*, **146**, 255–259.
Permi, P. (2001) *J. Magn. Reson.*, **153**, 267–272.
Permi, P. (2002) *J. Biomol. NMR*, **22**, 27–35.
Permi, P. (2003) *J. Biomol. NMR,*, **27**, 341–349.
Permi, P., and Annila, A. (2004) *Prog. NMR spectrosc.*, **44**, 97–137.
Prestegard, J.H., Al-Hashimi, H.M., and Tolman, J.R. (2000) *Quart. Rev. Biophys.*, **33**, 371–424.
Prestegard, J.H., Bougalt, C.M., and Kishore, A.L. (2004) *Chem. Rev.*, **104**, 3519–3540.
Tjandra, N., and Bax, A. (1997) *Science*, **278**, 1111–1114.
Vuister, G., and Bax, A. (1992) *J. Biomol. NMR*, **2**, 401–405.
Yang, D., Tolman, J.R., Goto, N.K., and Kay, L.E. (1998) *J. Biomol. NMR*, **12**, 325–332.
Yang, D., Venters, R.A., Mueller, G.A., Choy, W.Y., and Kay, L.E. (1999) *J. Biomol. NMR*, **14**, 333–343.
Zweckstetter, M., and Bax, A. (2000) *J. Am. Chem. Soc.*, **122**, 3791–3792.